The temperature and composition of the mantle sources of Martian basalts

Max Collinet[1], Ana-Catalina Plesa[1], Thomas Ruedas[2], Sabrina Schwinger[1], and Doris Breuer[1]

[1]German Aerospace Center
[2]Museum für Naturkunde Berlin

March 26, 2023

Abstract

The composition of basaltic melts in equilibrium with the mantle can be determined for several Martian meteorites and in-situ rover analyses. We use the melting model MAGMARS to reproduce these primary melts and estimate the bulk composition and temperature of the mantle regions from which they originated. We find that most mantle sources are depleted in CaO and Al2O3 relative to models of the bulk silicate Mars and likely represent melting residues or magma ocean cumulates. The concentrations of Na2O, K2O, P2O5, and TiO2 are variable and often less depleted, pointing to the re-fertilization of the sources by fluids and low-degree melts, or the incorporation of residual trapped melts during the crystallization of the magma ocean. The mantle potential temperatures of the sources are 1400-1500 ºC, regardless of the time at which they melted and within the range of the most recent predictions from thermochemical evolution models.

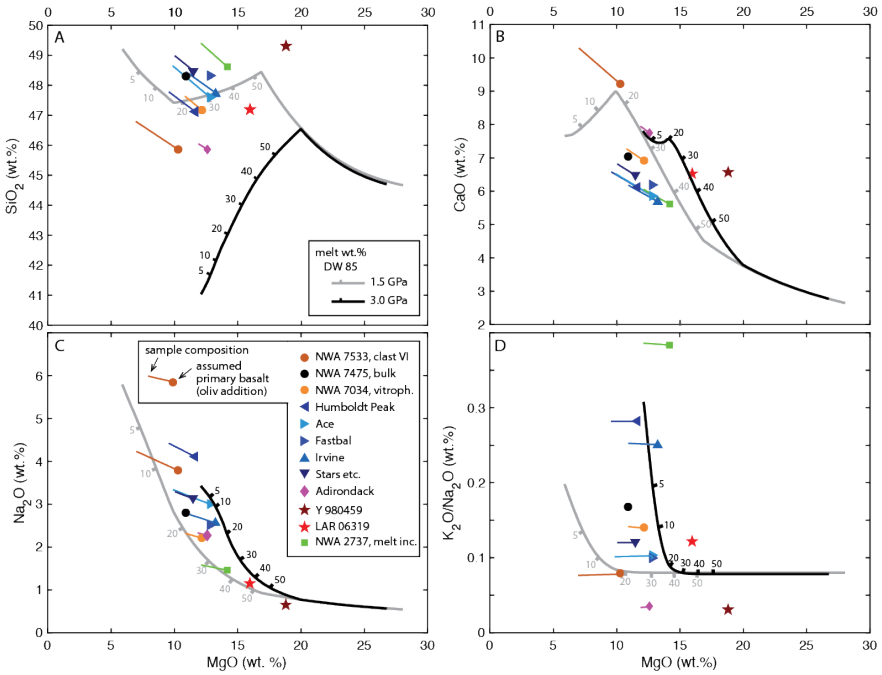

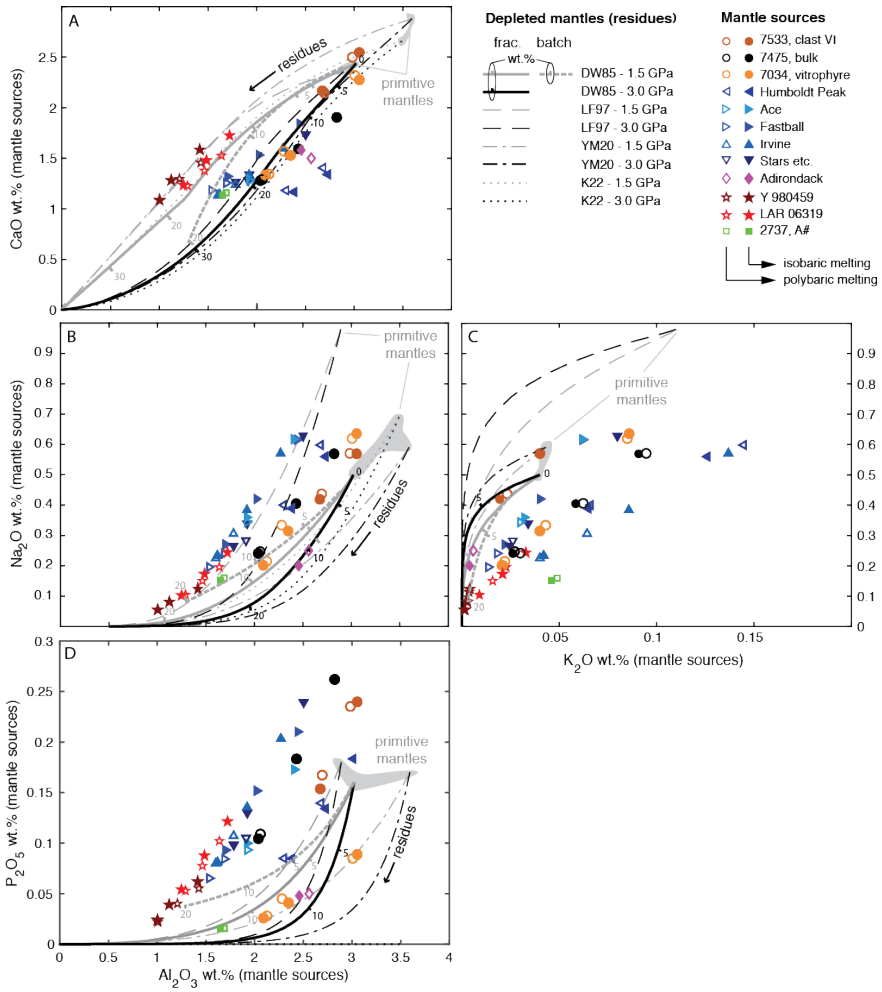

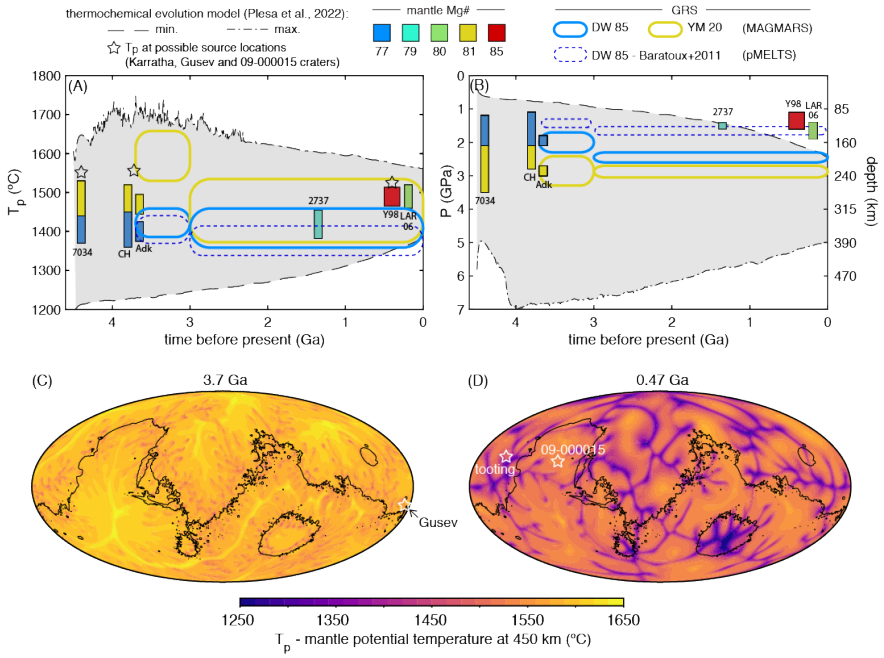

The temperature and composition of the mantle sources of Martian basalts

Max Collinet[1], Ana-Catalina Plesa[1], Thomas Ruedas[2,1], Sabrina Schwinger[1], and Doris Breuer[1]

[1]German Aerospace Center (DLR), Institute of Planetary Research, Rutherfordstraße 2, 12489 Berlin, Germany
[2]Museum für Naturkunde Berlin, Impact and Meteorite Research, Invalidenstraße 43, 10115 Berlin, Germany

Key Points:

- Basalts that sampled discrete mantle regions throughout Mars's history provide information about the mantle composition and temperature
- The mantle potential temperature of primitive basalts appears constant (1400–1500 ℃), yet is likely not representative of the average mantle
- Incompatible element concentrations in the mantle vary due to magma ocean crystallization, partial melting and metasomatism

Corresponding author: Max Collinet, `max.collinet@dlr.de`

Abstract

The composition of basaltic melts in equilibrium with the mantle can be determined for several Martian meteorites and in-situ rover analyses. We use the melting model MAGMARS to reproduce these primary melts and estimate the bulk composition and temperature of the mantle regions from which they originated. We find that most mantle sources are depleted in CaO and Al_2O_3 relative to models of the bulk silicate Mars and likely represent melting residues or magma ocean cumulates. The concentrations of Na_2O, K_2O, P_2O_5 and TiO_2 are variable and often less depleted, pointing to the re-fertilization of the sources by fluids and low-degree melts, or the incorporation of residual trapped melts during the crystallization of the magma ocean. The mantle potential temperatures of the sources are 1400–1500 ℃, regardless of the time at which they melted and within the range of the most recent predictions from thermochemical evolution models.

Plain Language Summary

Martian meteorites and rocks analyzed by rovers are witnesses of magmatic processes on Mars. In this study, we use the mantle melting model MAGMARS to determine the composition and temperature of the mantle regions from which primitive basalts have originated. Primitive basalts are closely related to mantle melts and hence record the properties of their mantle source. We find that the mantle compositions needed to explain these melts were poor in CaO and Al_2O_3. They likely represent a mantle that melted on several occasions or that crystallized from an early magma ocean. The composition of these primitive basalts indicates that some elements (Na_2O, K_2O, P_2O_5 and TiO_2) were subsequently added to the mantle source by fluids and low-degree melts. Alternatively, these elements can be explained by the trapping of melts during the evolution and progressive crystallization of the magma ocean. The temperature of the mantle sources projected to the surface conditions for easier comparison, (i.e., potential temperature) was 1400–1500 ℃, regardless of the time at which these sources melted and is within the range of the most recent predictions from planetary-scale models of interior dynamics.

1 Introduction

Our knowledge of the thermal state, composition and structure of the Martian mantle is derived from a diverse and continuously expanding array of geophysical and geochemical constraints. Early measurements of the moment of inertia factor, soil compositions at the Viking landing sites, and the definitive recognition that the "SNC meteorites" are from Mars (Baird et al., 1976; Johnston & Toksöz, 1977; Bogard & Johnson, 1983), unequivocally pointed to a FeO-rich mantle (Mg/(Fe+Mg)×100 in moles or Mg# = 75–81) compared to Earth (90). Model compositions of the "primitive mantle" were rapidly put forth (e.g., Dreibus & Wänke, 1985) and allowed to create simple models of the Martian interior structure (Longhi et al., 1992; Bertka & Fei, 1997; Elkins-Tanton et al., 2003). Additional analyses of crustal rocks by subsequent orbiting probes and rovers, the discovery of new Martian meteorites (Agee et al., 2013; Humayun et al., 2013), geodetic and seismic data from the recent InSight mission (e.g., Khan et al., 2021; Huang et al., 2022), and geodynamic modeling (e.g., Plesa et al., 2022), are now allowing to draw ever improving representations of the interior structure of Mars and its evolution through time.

Currently available compositions of the Martian mantle (e.g., Dreibus & Wänke, 1985; Lodders & Fegley, 1997; Yoshizaki & McDonough, 2020; Khan et al., 2022, abbreviated as DW85, LF97, YM20 and K22 hereinafter) represent average and idealized primitive compositions that are useful to derive average characteristics (density, solidus temperature, seismic wave velocity, etc.) but that probably do not represent actual regions of the mantle. The study of Martian meteorites has long shown that the mantle is highly

heterogeneous—both in terms of isotopic composition and Mg#—and suggests that a significant portion of the crust was formed very early (20–100 Myr; e.g., Borg et al., 1997; Debaille et al., 2008; Humayun et al., 2013; Nyquist et al., 2016; Kruijer et al., 2017; Bouvier et al., 2018) during (or briefly after) the crystallization of a Martian Magma Ocean (MMO). However, the major-element composition of the mantle reservoirs formed during the early differentiation of Mars is poorly constrained and model-dependent (e.g., Borg & Draper, 2003; Elkins-Tanton et al., 2005).

To derive more detailed models of the interior structure of Mars, independent constraints on the composition and temperature of discrete regions of the Martian mantle are desirable. A subset of Martian basalts, characterized by varied crystallization ages and high Mg# have been suggested to represent primitive basalts in near-equilibrium with their mantle sources and have been used to determine the P–T conditions of their mantle source through experiments (Musselwhite et al., 2006; Monders et al., 2007; Filiberto et al., 2008; Filiberto, Dasgupta, et al., 2010; Filiberto, Musselwhite, et al., 2010) or modeling (Lee et al., 2009; Filiberto & Dasgupta, 2011, 2015; Filiberto, 2017; Baratoux et al., 2011; Balta & McSween, 2013a). Most of these basalts cannot be produced by melting the primitive mantle and are instead expected to derive from mantle sources of diverse compositions (e.g., Schmidt & McCoy, 2010; Collinet et al., 2015, Fig. 1).

Here, we use MAGMARS, a new model developed to simulate melting in the Martian mantle (Collinet et al., 2021), to re-evaluate the melting conditions and the thermal state of the mantle sources of primitive Martian basalts, which crystallized at different times and therefore represent snapshots of Mars' thermochemical evolution. In addition, MAGMARS allows us to estimate for the first time the major-element composition of these local mantle sources. We find that the P–T melting conditions appear to have remained relatively stable through time and that mantle sources display variable CaO/Al_2O_3, low overall abundances of incompatible elements but enrichment of alkalis, P and Ti relative to Ca and Al. We discuss the implications of these findings for the early differentiation of Mars and its long-lived magmatism.

2 Selected compositions of primitive Martian basalts

While the majority of mantle melts were modified by igneous differentiation as they ascended through the crust (Udry et al., 2018; Payré et al., 2020; Ostwald et al., 2022; Farley et al., 2022; Wiens et al., 2022), a limited number of Martian basalts bear witness to the composition and temperature of the mantle at the time of their formation (i.e., primitive basalts). To identify primitive basalts, we first make the assumption that the average Martian mantle contains olivine Mg# $\geq$ 77 (Table 1, Table S1 and Fig. 1), and would produce primary melts with a Mg# $\geq$ 54 ($K_{D,\,\mathrm{Fe-Mg}}^{\mathrm{oliv-liq}}$ of 0.35; Filiberto & Dasgupta, 2011). A mantle of Mg# 77 is intermediate between the most commonly accepted primitive mantle compositions (Dreibus & Wänke, 1985; Yoshizaki & McDonough, 2020). Here, we only consider martian basaltic compositions with a Mg# $\geq$ 48, which could derive from primary mantle melts of Mg# $\geq$ 54 following a maximum of 10 wt.% of olivine fractionation.

The Spirit rover analyzed numerous basalts with Mg# 48–55 at Gusev crater (McSween, Wyatt, et al., 2006; Squyres et al., 2007; Ming et al., 2008) that could represent primitive basalts (Monders et al., 2007; Filiberto, Dasgupta, et al., 2010; Schmidt & McCoy, 2010). Among these, the Adirondack-class basalts are poor in K_2O and could derive from a residual mantle depleted in incompatible elements by prior melting events (Schmidt & McCoy, 2010; Collinet et al., 2021) while most of the basalts analyzed in the vicinity of the Columbia Hills are more enriched in alkali elements and poorer in CaO (Fig. 1). The ancient regolith breccia NWA 7034/7475/7533 (Humayun et al., 2013; Nyquist et al., 2016; Cassata et al., 2018; Bouvier et al., 2018) is also characterized by a high Mg# (54; Wittmann et al., 2015) and, despite its complex history, could approach the com-

position of a mantle melt based on trace (Humayun et al., 2013) and major element compositions (Collinet et al., 2015). We also test whether two individual clasts could be representative of primitive basalts later remelted by impacts: a vitrophyre (Udry et al., 2014) and an alkali-rich microbasalt known as "Clast VI" (Humayun et al., 2013).

Recent geophysical constraints suggest that large portions of the mantle could be more Mg-rich (Mg# = 81; Khan et al., 2022) than previously assumed (e.g., Dreibus & Wänke, 1985; Yoshizaki & McDonough, 2020), as also evidenced by the study of Martian meteorites. The most primitive depleted shergottite (Yamato 980459, nearly identical to NWA 5789; Greshake et al., 2004; Gross et al., 2011) and the most primitive enriched shergottite (LAR 06319, nearly identical to NWA 1068; Barrat et al., 2002; Peslier et al., 2010) have Mg# of 66 and 58, respectively. Y 980459 contains olivine Mg# 85–86 and is thought to represent a primary melt composition (e.g., Musselwhite et al., 2006; Matzen et al., 2022). The olivine megacrysts in LAR 06319 and NWA 1068 have Mg# $\leq$ 77 (Basu Sarbadhikari et al., 2009) but were initially more magnesian (Mg# 80) and were modified by Fe–Mg diffusion (Balta et al., 2013; Collinet et al., 2017). NWA 2737 is a dunitic cumulate (Mg# 79) with olivine-hosted melt inclusions. Its primary melt is taken as the reconstructed composition of the parental trapped liquid (PTL; He et al., 2013). Given the multitude of evidence of Mg-rich mantle reservoirs, we also calculated alternative primary melt compositions for the Gusev basalts and NWA 7034/7475/7533 bulk rock and basaltic clasts that would be in equilibrium with a Mg# of 81. In this case, larger amounts of olivine have to be added to the parental melt compositions (Table 1).

Table 1. List of Martian primitive basalts, fraction of olivine addition required to reach mantle-melt equilibrium, and associated inferred mantle Mg#

		age (Ga)	oliv (wt.%)	Mg#
NWA 7034	Vitrophyre [1]	4.49 [2]	+10 / +26	77 / 81
NWA 7533	Clast VI [3]	4.49 [2]	+9 / +24	77 / 81
NWA 7475	bulk [4]	4.49 [2]	0	77
Adirondack-class basalts [5]		3.7 [6]	+3 / +17	77 / 81
Columbia Hills	Humboldt Peak [7]	3.7 [6]	+7 / + 20	77 / 81
	Fastball [8]	3.7 [6]	0 / +13	77 / 81
	Stars, etc. [8]	3.7 [6]	+5 / +17	77 / 81
	Ace [8]	3.7 [6]	+9 / +29	77 / 81
	Irvine [7]	3.7 [6]	+8 / +25	77 / 81
chassignite	NWA 2737 [9]	1.3 [10]	+9	79
depleted shergottite	Y 980459 [11]	0.47 [12]	0 / +7	85 / 86
enriched shergottite	LAR 06319 [13]	0.19 [14]	0 / +5	80 / 81

[1] Udry et al. (2014), [2] Costa et al. (2020), [3] Humayun et al. (2013), [4] Wittmann et al. (2015)
[5] McSween, Wyatt, et al. (2006), [6] Greeley et al. (2005), [7] Ming et al. (2008)
[8] Squyres et al. (2007), [9] He et al. (2013), [10] Udry and Day (2018)
[11] average of Misawa (2004), Shirai and Ebihara (2004) and Greshake et al. (2004)
[12] Shih et al. (2005), [13] Basu Sarbadhikari et al. (2009), [14] Shafer et al. (2010)

3 Methods

To constrain the mantle sources of the target basaltic compositions described above (Table 1 and S1), we first simulate the melting of various primitive mantle compositions (DW85, YM20 and K22) using MAGMARS (Collinet et al., 2021). We then adjust the mantle compositions incrementally (Mg#, TiO_2, Al_2O_3, CaO, Na_2O, K_2O, and P_2O_5 concentrations) until the liquids produced are identical to the target compositions (i.e.,

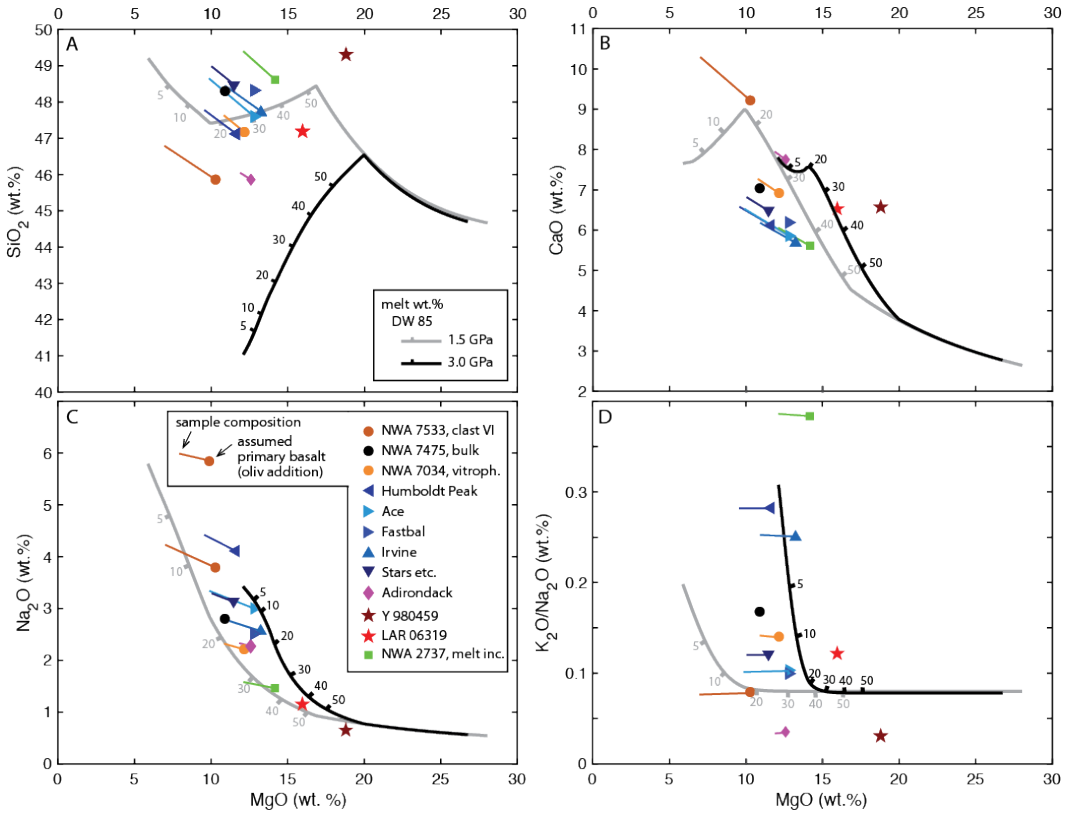

Figure 1. Comparison between the composition of Martian primitive basalts (left extremity of colored lines), their recalculated primary melts (symbols) and the melts produced by melting of the primitive mantle of Dreibus and Wänke (1985) at 1.5 (grey line) and 3.0 GPa (black line), as calculated by MAGMARS. The high SiO_2 content of primary melts (A) is consistent with shallow melting conditions ($\ll$ 3.0 GPa). But compared to shallow DW85 melts (1.5 GPa), many primary basalts have either lower or higher CaO contents (B) and higher Na_2O and K_2O contents (C-D), and must therefore derive from mantle sources of contrasting compositions.

when the concentrations of all major and incompatible elements are within 1 wt.% relative). Next, we mathematically remove a fraction (33 to 50 wt.%) of the melt (of composition identical to the target compositions) and repeat the same procedure to identify more refractory mantle compositions that can still produce identical melts. This approach, in the absence of independent constraints on the melt fraction, leads to the identification of several possible mantle sources for each target composition. To discuss the non-uniqueness of the sources and quantify model uncertainties for the Fastball primary melt (representative example), we performed ∼500000 MAGMARS calculations by randomly varying the parameters around their average values. This automated search identified slightly larger compositional trends compared to the manual search. However, the mantle sources identified manually were found sufficient to discuss the mantle source origin and melting temperature. It is this dataset (Table S2) that is described in the following sections.

4 Results

The compositions of the mantle sources that can produce melts identical to the target primary basalts (Table 1 and Fig. 1) are shown in Figure 2 and reported in Table S2. Each primary basalt composition can be matched by melting a series of mantle sources characterized by various concentrations of incompatible elements (Al_2O_3, CaO, Na_2O, K_2O), both isobarically and polybarically. Despite the non-uniqueness of solutions, first-order chemical differences between the sources of the different basaltic compositions can be identified. For example, the possible sources of shergottites are all notably poorer in Al_2O_3 and Na_2O than the sources of the Gusev basalts (Fig. 2a). Among the latter, the sources of the Columbia Hills basalts are characterized by high Na_2O, K_2O, and P_2O_5 concentrations (Fig. 2b–d) compared to the source of the Adirondack basalts. The source of the NWA 2737 chassignite shows the highest K_2O/Na_2O ratio. Finally, one of the sources that can match the composition of Clast VI (NWA 7533) is nearly identical to the DW85 primitive mantle.

The melt fractions required to produce the primary basalt compositions are comprised between 5 and 30 wt.%. The associated mantle potential temperatures (T_p) are between 1320 and 1520 ℃ (Fig. 3a and Table S2). The average pressure of melting is relatively low for all samples (1.1–2.0 GPa), and is largely constrained by the SiO_2 and MgO concentrations of the target primary melts (Fig. 1a). If a Mg# of 81 (K22) is assumed instead of 77 for NWA 7034/7475/7533 and Gusev basalts, then the primary basalts would contain a larger olivine component and the mantle T_p (1390–1570 ℃) and average pressure of melting (1.9–3.0 GPa) would both be higher (Fig. 3).

5 Discussion

5.1 Thermal state of the Martian mantle

Compared to the T_p estimates of Filiberto (2017), and using the same starting assumptions (mantle of Mg# 77 and batch melting), we find that Gusev crater basalts are derived from slightly cooler mantle sources on average, with T_p of ∼1400 ℃ (vs. ∼1450 ℃), but that the ranges of possible T_p largely overlap (1360–1460 vs. 1390–1550 ℃, respectively). Allowing for a higher Mg# of the mantle sources (77–81), we find that Gusev basalts and all (pre-)Noachian to Hesperian samples point to a T_p of 1340–1520 ℃ (Fig. 3a).

We calculate a T_p of 1420–1430 ℃ for the primary melt composition reconstructed from NWA 2737 melt inclusions (He et al., 2013), assumed to be parental to the middle-Amazonian nakhlites and chassignites (1.34 Ga; Udry & Day, 2018). However, the mantle source could have been metasomatized (Day et al., 2018, also see section 5.2) and could

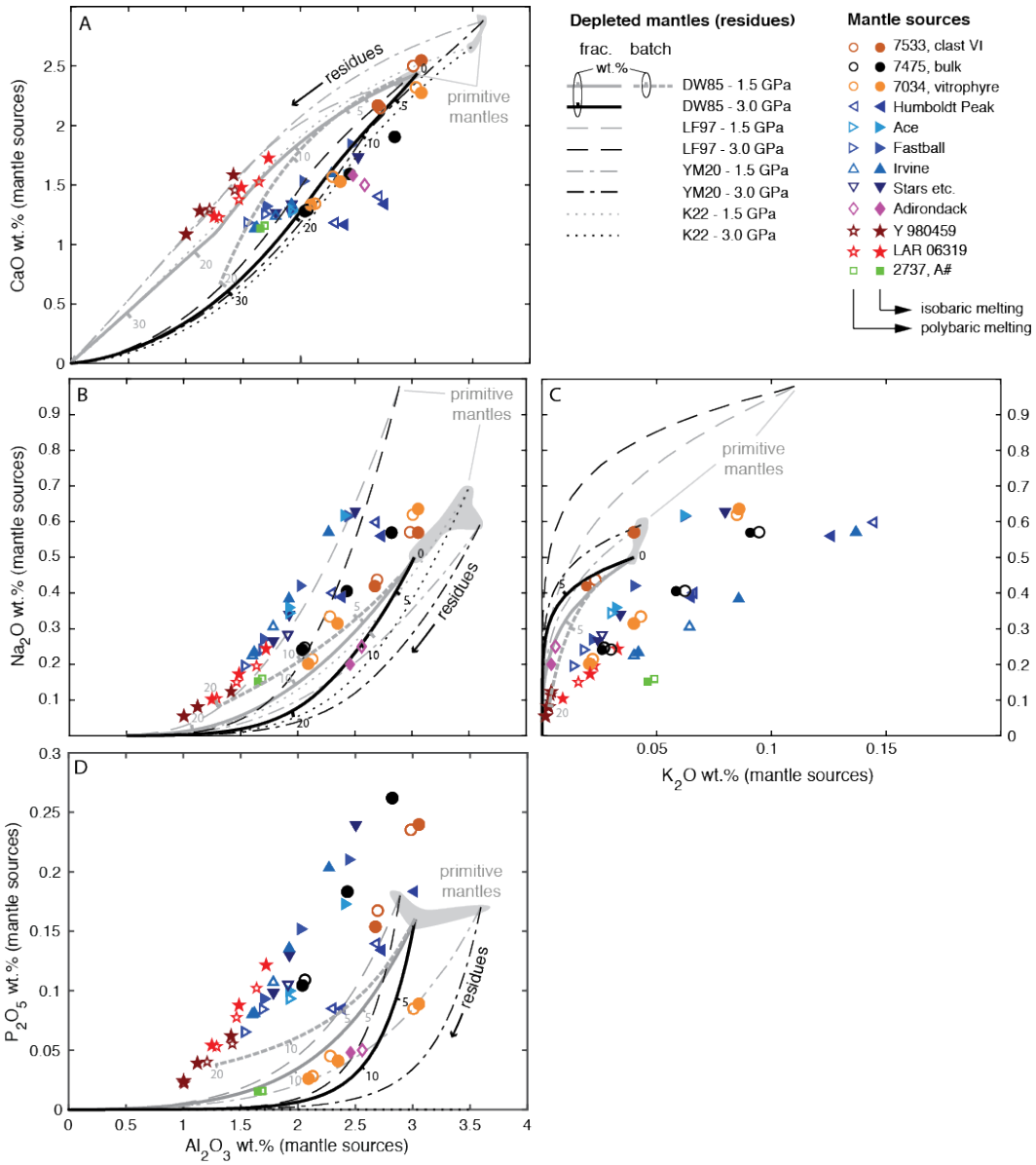

Figure 2. Incompatible element concentrations of the mantle sources of primary basalts (symbols) compared to residual model Martian mantles (lines). Each line represents the trajectory of residues produced by progressive melting of a primitive mantle composition (apex) at 1.5 (grey) and 3.0 GPa (black). For the DW85 model (solid lines), tick marks indicate the composition of residues after specific degrees of melting (in wt.%). All mantle source compositions are relatively poor in CaO and Al_2O_3 compared to the primitive mantle and are characterized by variable CaO/Al_2O_3 (A). The source of NWA 7533 clast VI is similar to a primitive mantle (DW85) and the source of the Adirondack basalts resemble a residual mantle following prior partial melting in all compositional spaces (A–D). All other sources are too rich in alkali elements—Na_2O (B) and especially K_2O (C)—and other incompatible elements, such as P_2O_5 (D), to derive from model Martian mantles by partial melting alone and other processes must be considered (see section 5.2).

have contained up to 250 ppm of water (McCubbin et al., 2016), which would translate into a lower T_p of 1380 ℃ (Katz et al., 2003).

The more recent olivine-phyric shergottites (160-500 Ma; Moser et al., 2013; Wu et al., 2021; McFarlane & Spray, 2022) are picritic basalts that have been linked to plumes with a T_p of at least 1480–1550 ℃ (e.g., Musselwhite et al., 2006; Filiberto & Dasgupta, 2015). The T_p of MAGMARS simulations (1470–1520 ℃) are within error of these previous constraints if batch melting is assumed, and slightly lower in the polybaric case (1440–1450 ℃). The presence of water in the source of shergottites could in principle lower the minimum T_p and has been suggested to account for their relatively high SiO_2 concentrations (Balta & McSween, 2013b). However, the small initial water concentration of the source (14–73 ppm; McCubbin et al., 2016) and the fact that the SiO_2 concentration of shergottite melts can be reproduced with MAGMARS under nominally anhydrous conditions preclude a significant effect of water.

Finally, we re-calculate using MAGMARS the T_p and pressures of melting of the bulk volcanic provinces of Baratoux et al. (2011), as constrained by the Gamma Ray Spectrometer (GRS) on board NASA's Mars Odyssey spacecraft. Baratoux et al. (2011) used pMELTS in their analysis, which has since been shown to overestimate FeO and underestimate SiO_2 concentrations by up to 8 wt.% (Collinet et al., 2021), significantly more than anticipated by El Maarry et al. (2009). For Hesperian provinces, while the ranges of T_p are similar (1390–1460 vs. 1370–1420 ℃ previously), MAGMARS predicts a slightly higher pressure of melting (1.6–2.3 vs. 1.3–1.6 GPa). However, we find that only Ascraeus and Elysium Mons (out of the 6 Amazonian volcanic provinces) can be matched with a DW85 mantle composition using MAGMARS (Table S3). The composition of the other 4 provinces can either not be reproduced at all (Arsia and Pavonis Mons) or only with an extremely small melt fraction of <2 wt.% (Olympus Mons and Alba Patera). With a YM20 composition (Mg# of 79, 81 after 15 wt.% of melting), a higher T_p of 1520–1660 ℃ and higher pressures of melting (2.3–3.5 GPa) are necessary to match the Hesperian volcanic provinces. A higher Mg# mantle also allows to reproduce the composition of a greater number of Amazonian volcanic provinces (5, all but Arsia Mons) with T_p of 1380–1460℃ and pressures of 2.8–3.1 GPa.

The lack of temperature and pressure trends over time displayed by this set of constraints renders it impossible to calculate rates of secular cooling or lithosphere thickening (Fig. 3a,b). This could be due to the limited number of primitive basalts available that might not be representative of the average mantle. To test this possibility, we compare the mantle temperature estimates derived from MAGMARS to the results of a global convection model incorporating the most recent interior structure constraints from InSight (Plesa et al., 2022). The maximum temperature (and minimum pressure) at which the mantle is melting decreases with time (i.e. secular cooling). However, at any given time, melt is produced from regions of the mantle with highly variable T_p, which encompass the T_p of the mantle sources estimated in this study. The Gusev basalts are the only primitive basalts whose location is known with certainty. Additionally, NWA 7034 and the depleted shergottites have recently been suggested to have originated from Karratha and 09-000015 craters, respectively (Lagain et al., 2021, 2022). Under all three locations and at the appropriate—and highly contrasting— crystallization ages, the T_p of the mantle sources would have been nearly identical and in the range 1525–1562 ℃ (Fig. 3c,d and S3). This confirms that despite the overall decrease in mantle temperature with time, a limited basaltic sample suite can record near-constant mantle temperature. The thermochemical evolution model predicts that the mantle temperature should first increase due to the decay of radioactive elements and peak at the Noachian/Hesperian transition before slowly decreasing (e.g., Plesa et al., 2022). This thermal maximum is not recorded by the 3.7 billion years old Gusev basalts but seems consistent with our reinterpretation of the T_p of Hesperian volcanic provinces (1520–1660 ℃; Baratoux et al.,

2011), assuming that the average mantle is relatively MgO-rich (Mg# of 79; Yoshizaki & McDonough, 2020).

Perhaps the main discrepancy between the thermochemical evolution model and the MAGMARS constraints is the shallow depth of melting that we estimate for the source of shergottites, which is predicted to be well within the lithospheric mantle (Plesa et al., 2022). Filiberto (2017) noted that if a larger amount of olivine fractionation had taken place, the primary melts of shergottites could have been in equilibrium with the convecting mantle at 3–5 GPa. While this pressure of melting is more consistent with the thick lithosphere of the late Amazonian (Fig. S3), such melt compositions would require a high T_p of 1710 ± 73 ℃, which exceeds significantly the maximum T_p achievable by thermal evolution models at that time (Fig. 3d). Therefore, we consider it more likely that the T_p of the sources was low (1470–1520 ℃) and that the pressure of melting derived from MAGMARS simulations (1.6 ± 0.5 GPa) does not represent the average pressure of melting but simply the final pressure of equilibration with the mantle. If shergottites formed in the Tharsis region (e.g., Lagain et al., 2021), deeply-sourced primary melts could have re-equilibrated with a warm lithospheric mantle, locally heated by magmas, at the base of the crust (110–130 km; Wieczorek et al., 2022).

5.2 Origin of the mantle sources and their variable concentrations of incompatible elements

The mantle source of Clast VI (NWA 7533) could be nearly identical to the primitive mantle (Fig. 2), as previously suggested based on rare-earth element (REE) modeling (Humayun et al., 2013). All other mantle sources are depleted in CaO and Al_2O_3 relative to the various primitive mantle compositions proposed in literature (DW85, LF97, YM20 and K22). One possibility is that these mantle sources represent melting residues from which 10–20 wt.% melt had been removed prior to producing the melts that eventually formed the primitive basalts used in this study (Fig. 2a). However, the concentrations of alkalis and other incompatible elements (e.g., TiO_2, P_2O_5) are, in most cases, too high at a given Al_2O_3 concentration, regardless of the style (batch vs. fractional) and pressure of melting (Fig. 2b–d). Only the Adirondack basalts are consistent in detail with the simple re-melting of a mantle residue, following ±10 wt.% prior melting of a primitive mantle (see also Collinet et al., 2021). Other processes must be invoked to explain the chemical variability of the remaining mantle sources.

The Columbia Hills basalts are often assumed to be related to the Adirondack basalts, as both groups were analyzed by Spirit at Gusev crater. Compared to the Adirondack basalts, they are rich in alkali elements as well as other incompatible elements (TiO_2, P_2O_5) and poor in CaO and Al_2O_3 (Fig. 1). McSween, Ruff, et al. (2006) suggested that the Columbia Hills basalts could have derived from melts similar to the Adirondack basalts by fractional crystallization. The higher incompatible element concentrations (e.g., K, P, Ti) of the Columbia Hills basalts have also been suggested to result from the contamination of Adirondack-like primitive melts by a crustal component (Schmidt & McCoy, 2010). However, crustal assimilation and fractional crystallization (AFC) of basaltic melts should lower markedly the MgO concentrations (and Mg#; Ostwald et al., 2022). As the Mg# of the Columbia Hills and Adirondack basalts are similar, most workers now regard them as two sets of near-primary melts (Schmidt & McCoy, 2010; Filiberto & Dasgupta, 2011; Collinet et al., 2015). Schmidt and McCoy (2010) proposed that the high K_2O content of the Columbia Hills basalts could be accounted for by melting a fertile mantle source with a higher K_2O content compared to the Dreibus and Wänke (1985) composition. According to their model, the Adirondack basalts would be slightly younger and produced by re-melting the same region of the mantle. However, the similarly low CaO and Al_2O_3 concentrations of their sources (Fig. 2a) suggest that both the Adirondack and Columbia Hills basalts were derived from depleted mantles, affected by 10–20 wt.% prior melting at ∼ 3.0 GPa. Metasomatism has been invoked to reconcile the high

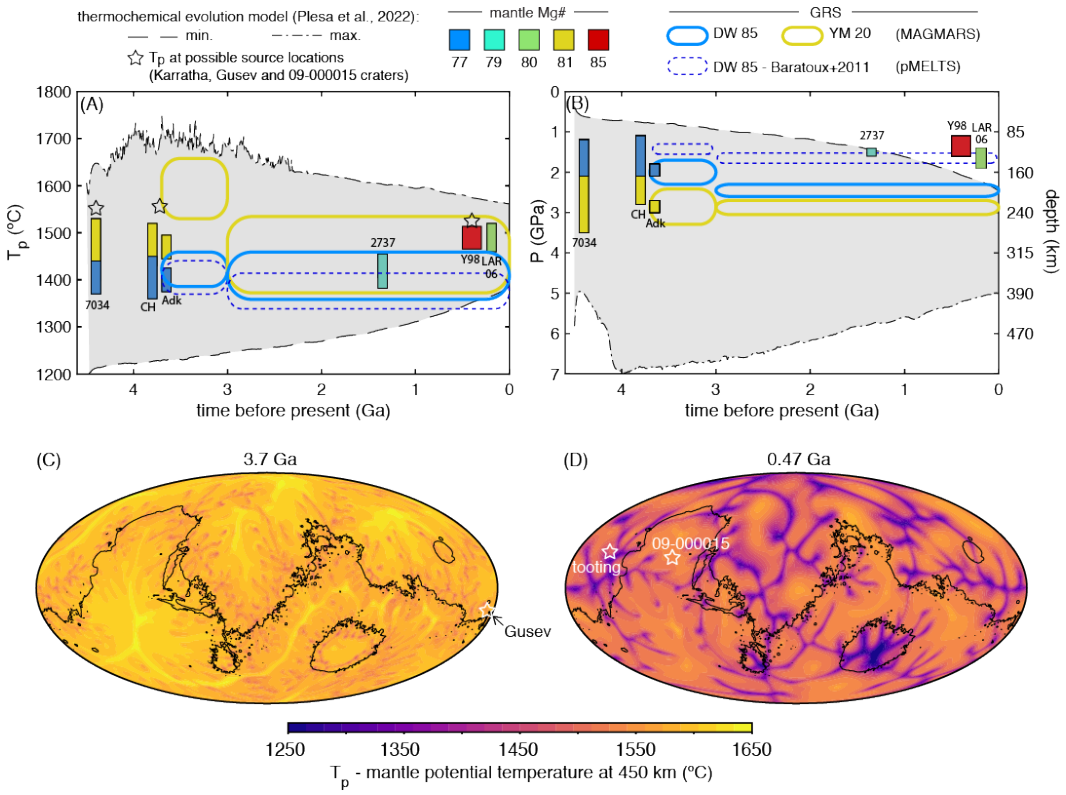

Figure 3. Temporal evolution of T_{p} (A) and the average pressure and depth of melting or conditions of mantle–melt re-equilibration (B). The rectangles represent the sources of the basaltic compositions listed in Table 1. The rounded fields are the sources of the GRS volcanic provinces of Baratoux et al. (2011), re-calculated with MAGMARS. The black lines represent the evolution of the potential temperatures and pressures of the part of the mantle that is affected by partial melting in the thick-crust geodynamical model of Plesa et al. (2022). The minimum pressure of melting (dashed line in B) can be interpreted as the thinnest thermal lithosphere observed anywhere on the planet. Panels C and D represent regional variations in T_{p} for this geodynamical model at the time of Gusev basalt (C) and depleted shergottites (D) crystallization. At their possible source locations (white stars, see text for references), the T_{p} are nearly identical: 1562 vs. 1525 °C (see also Fig. S3).

water and incompatible element concentrations of nakhlites-chassignites with their Sr-Nd isotopic compositions indicative of ancient depleted sources (Goodrich et al., 2013; McCubbin et al., 2013; Day et al., 2018) and could also help explain the high K_2O concentrations analyzed in numerous rocks from Gale crater (e.g., Schmidt et al., 2014). Similarly, we posit that the relative enrichment of incompatible elements in the Columbia Hills basalts (alkali elements as well as elements like P and Ti that are less mobile in fluids) could be explained by the secondary addition of low-degree melts to a Adirondack-like mantle source. The highest possible K_2O concentrations that we calculate for the Columbia Hills mantle sources are in the range 0.13–0.15 wt.%. This is much smaller than the percent level K_2O concentrations of highly metasomatized and phlogopite-bearing terrestrial peridotites (e.g., Condamine & Médard, 2014) but similar to other intraplate peridotites containing no hydrous phases (e.g., Smith et al., 1993). The source of the Columbia Hills basalts was likely affected by low degrees of cryptic metasomatism and was thus not significantly hydrated.

The isotopic systematics of Martian meteorites suggest the existence of a magma ocean that crystallized early in Mars' history (e.g., Elkins-Tanton et al., 2005; Debaille et al., 2008; Kruijer et al., 2017; Bouvier et al., 2018). Some of the resulting heterogeneity was never erased by convection and ancient mantle sources were affected by partial melting and formed the shergottites as recently as 170 million years ago (Moser et al., 2013; Wu et al., 2021; McFarlane & Spray, 2022). The major and incompatible element concentrations of the sources of shergottites must in part reflect the processes of magma ocean crystallization. For example, the superchondritic CaO/Al_2O_3 ratio of shergottites has been suggested to result from the fractionation of majorite in the deep mantle (Borg & Draper, 2003). Here, we find that the sources of shergottites had mildly superchondritic CaO/Al_2O_3 ratios that could have appeared at low pressure, following 15–20 wt.% melting of the primitive mantle (Fig. 2a). A 20 wt.% depletion from a primitive mantle is also sufficient to decrease the incompatible element concentrations to levels identical to those of the source of depleted shergottites (Fig. 2b–d). In this case, however, the melting residue only reaches a Mg# of 77 (when starting from a DW85 mantle) to 81 (YM20), following 20 wt.% of melting. The much higher Mg# of the source of Y 980659 (85–86) remains easier to explain if it formed as a magma ocean cumulate (e.g., Borg & Draper, 2003; Elkins-Tanton et al., 2005). The enriched shergottites have higher concentrations of incompatible elements. Their composition in radiogenic isotopes indicates that the enriched signature is most likely derived from evolved residual melts that were trapped in mantle cumulates during the crystallization of an early MMO, rather than from crustal assimilation (e.g., Borg & Draper, 2003; Symes et al., 2008; Debaille et al., 2008; Brandon et al., 2012; Ferdous et al., 2017; Armytage et al., 2018). This could also explain the slightly higher concentrations of minor incompatible elements that we calculate for the source of enriched shergottites (Fig. 2).

6 Conclusions

The mantle temperature of the sources that gave rise to known primitive basalts appears to have remained relatively stable through time (T_p of 1400–1500 ℃). This could be due to a sampling bias. The higher mantle T_p (∼1600 ℃) of the Hesperian volcanic provinces (Baratoux et al., 2011), recalculated with MAGMARS and assuming a mantle with Mg# of 79 or higher (Yoshizaki & McDonough, 2020; Khan et al., 2022), hint at a significant secular cooling (>100 ℃) as expected from thermochemical evolution models (Plesa et al., 2022). The shergottite melts were likely produced at pressures greater than 3 GPa but re-equilibrated with the lithospheric mantle at 1–2 GPa, for example at the base of the thick Tharsis crust.

With the exception of the source of NWA 7034 and paired rocks, the mantle sources of known Martian basalts were poorer in Al_2O_3 and CaO compared to primitive mantle compositions (e.g., Dreibus & Wänke, 1985; Yoshizaki & McDonough, 2020). The com-

positions of the sources of Gusev crater basalts that we calculate do not explicitly require a magma ocean stage and could represent simple depleted mantle reservoirs affected by 10–20 wt.% prior melting (Adirondack basalts) or depleted mantle reservoirs re-fertilized by fluids and low-degree silicate melts (Columbia Hills basalts). On the other hand, the major element composition of the source of depleted shergottites cannot be easily explained by partial melting alone and suggest, along with their Sr-Nd-Hf isotope systematics, that they formed as mantle cumulates during the crystallization of the MMO. The sources of enriched shergottites are consistent with trapping a more evolved residual melt. It is also possible that the relative enrichment of the minor incompatible elements (Na, K, Ti and P) of the Columbia basalts is a vestige of magma ocean processes and does not result from metasomatism. But regardless of its origin, this relative enrichment is limited, with concentrations of Na_2O, P_2O_5, and TiO_2 not exceeding the range displayed by primitive mantle compositions.

Acknowledgments

M.C. and A.C.P. gratefully acknowledge the financial support and endorsement from the DLR Management Board Young Research Group Leader Program and the Executive Board Member for Space Research and Technology. M.C. and S.S. were supported by DFG (Deutsche Forschungsgemeinschaft) from the DFG programme SFB-TRR 170. T.R. was supported by DFG grant Ru 1839/2-1. This is TRR 170 publication no. 187. We thank xxx and xxx.

Open Research

The data used for the discussion and figures is summarized in the supplementary material (Table S1-S3) and available in full at https://doi.org/10.5281/zenodo.7691390 (Collinet et al., 2023)

References

Agee, C. B., Wilson, N. V., McCubbin, F. M., Ziegler, K., Polyak, V. J., Sharp, Z. D., ... Elardo, S. M. (2013). Unique Meteorite from Early Amazonian Mars: Water-Rich Basaltic Breccia Northwest Africa 7034. *Science*. doi: 10.1126/science.1228858

Armytage, R. M., Debaille, V., Brandon, A. D., & Agee, C. B. (2018). A complex history of silicate differentiation of Mars from Nd and Hf isotopes in crustal breccia NWA 7034. *Earth and Planetary Science Letters*, *502*, 274–283. doi: 10.1016/j.epsl.2018.08.013

Baird, A. K., Toulmin, P., Clark, B. C., Rose, H. J., Keil, K., Christian, R. P., & Gooding, J. L. (1976). Mineralogic and petrologic implications of Viking geochemical results from Mars: Interim report. *Science*, *194*(4271), 1288–1293. doi: 10.1126/science.194.4271.1288

Balta, J. B., & McSween, H. Y. (2013a). Application of the MELTS algorithm to Martian compositions and implications for magma crystallization. *Journal of Geophysical Research: Planets*, *118*(12), 2502–2519. doi: 10.1002/2013JE004461

Balta, J. B., & McSween, H. Y. (2013b). Water and the composition of Martian magmas. *Geology*. doi: 10.1130/g34714.1

Balta, J. B., Sanborn, M., McSween, H. Y., & Wadhwa, M. (2013). Magmatic history and parental melt composition of olivine-phyric shergottite LAR 06319: Importance of magmatic degassing and olivine antecrysts in Martian magmatism. *Meteoritics and Planetary Science*, n/a–n/a. doi: 10.1111/maps.12140

Baratoux, D., Toplis, M. J., Monnereau, M., & Gasnault, O. (2011). Thermal history of Mars inferred from orbital geochemistry of volcanic provinces. *Nature*,

472(7343), 338–41. doi: 10.1038/nature09903

Barrat, J. A., Jambon, A., Bohn, M., Gillet, P., Sautter, V., Gopel, C., ... Keller, F. (2002). Petrology and chemistry of the picritic shergottite North West Africa 1068 (NWA 1068). *Geochimica Et Cosmochimica Acta*, *66*(19), 3505–3518.

Basu Sarbadhikari, A., Day, J. M., Liu, Y., Rumble, D., & Taylor, L. a. (2009). Petrogenesis of olivine-phyric shergottite Larkman Nunatak 06319: Implications for enriched components in martian basalts. *Geochimica et Cosmochimica Acta*, *73*(7), 2190–2214. doi: 10.1016/j.gca.2009.01.012

Bertka, C. M., & Fei, Y. (1997). Mineralogy of the Martian interior up to core-mantle boundary pressures. *J. Geophys. Res.*, *102*(B3), 5251–5264. doi: 10.1029/96jb03270

Bogard, D. D., & Johnson, P. (1983). Martian gases in an antarctic meteorite? *Science*, *221*(4611), 651–654. doi: 10.1126/science.221.4611.651

Borg, L. E., & Draper, D. S. (2003). A petrogenetic model for the origin and compositional variation of the martian basaltic meteorites. *Meteoritics and Planetary Science*, *38*(12), 1713–1731.

Borg, L. E., Nyquist, L. E., Taylor, L. A., Wiesmann, H., & Shih, C. Y. (1997). Constraints on Martian differentiation processes from Rb-Sr and Sm-Nd isotopic analyses of the basaltic shergottite QUE 94201. *Geochimica et Cosmochimica Acta*, *61*(22), 4915–4931. doi: 10.1016/S0016-7037(97)00276-7

Bouvier, L. C., Costa, M. M., Connelly, J. N., Jensen, N. K., Wielandt, D., Storey, M., ... Bizzarro, M. (2018). Evidence for extremely rapid magma ocean crystallization and crust formation on Mars. *Nature*, *558*(7711), 586–589. doi: 10.1038/s41586-018-0222-z

Brandon, A. D., Puchtel, I. S., Walker, R. J., Day, J. M., Irving, A. J., & Taylor, L. a. (2012). Evolution of the martian mantle inferred from the 187Re–187Os isotope and highly siderophile element abundance systematics of shergottite meteorites. *Geochimica et Cosmochimica Acta*, *76*, 206–235. doi: 10.1016/j.gca.2011.09.047

Cassata, W. S., Cohen, B. E., Mark, D. F., Trappitsch, R., Crow, C. A., Wimpenny, J., ... Smith, C. L. (2018). Chronology of martian breccia NWA 7034 and the formation of the martian crustal dichotomy. *Science Advances*, *4*(5). doi: 10.1126/sciadv.aap8306

Collinet, M., Charlier, B., Namur, O., Oeser, M., Médard, E., & Weyer, S. (2017). Crystallization history of enriched shergottites from Fe and Mg isotope fractionation in olivine megacrysts. *Geochimica et Cosmochimica Acta*, *207*, 277–297. doi: 10.1016/j.gca.2017.03.029

Collinet, M., Médard, E., Charlier, B., Vander Auwera, J., & Grove, T. L. (2015). Melting of the primitive martian mantle at 0.5–2.2 GPa and the origin of basalts and alkaline rocks on Mars. *Earth and Planetary Science Letters*, *427*(0), 83–94. doi: http://dx.doi.org/10.1016/j.epsl.2015.06.056

Collinet, M., Plesa, A., Grove, T. L., Schwinger, S., Ruedas, T., & Breuer, D. (2021). MAGMARS: A Melting Model for the Martian Mantle and FeO-Rich Peridotite. *Journal of Geophysical Research: Planets*, *126*(12), e2021JE006985. doi: 10.1029/2021je006985

Collinet, M., Plesa, A.-C., Ruedas, T., Schwinger, S., & Breuer, D. (2023). *The temperature and composition of the mantle sources of Martian basalts [dataset+software].* Zenodo. doi: 10.5281/zenodo.7691390

Condamine, P., & Médard, E. (2014). Experimental melting of phlogopite-bearing mantle at 1 GPa: Implications for potassic magmatism. *Earth and Planetary Science Letters*, *397*(0), 80–92. doi: http://dx.doi.org/10.1016/j.epsl.2014.04.027

Costa, M. M., Jensen, N. K., Bouvier, L. C., Connelly, J. N., Mikouchi, T., Horstwood, M. S., ... Bizzarro, M. (2020). The internal structure and

geodynamics of Mars inferred from a 4.2-Gyr zircon record. *Proceedings of the National Academy of Sciences of the United States of America*, *117*(49), 30973–30979. doi: 10.1073/pnas.2016326117

Day, J. M. D., Tait, K. T., Udry, A., Moynier, F., Liu, Y., & Neal, C. R. (2018). Martian magmatism from plume metasomatized mantle. *Nature Communications*, *9*(1), 4799. doi: 10.1038/s41467-018-07191-0

Debaille, V., Yin, Q.-Z., Brandon, A., & Jacobsen, B. (2008). Martian mantle mineralogy investigated by the 176Lu–176Hf and 147Sm–143Nd systematics of shergottites. *Earth and Planetary Science Letters*, *269*(1-2), 186–199. doi: 10.1016/j.epsl.2008.02.008

Dreibus, G., & Wänke, H. (1985). Mars, a volatile-rich planet. *Meteoritics*, *20*(2), 367–381.

El Maarry, M., Gasnault, O., Toplis, M., Baratoux, D., Dohm, J., Newsom, H., ... Karunatillake, S. (2009). Gamma-ray constraints on the chemical composition of the martian surface in the Tharsis region: A signature of partial melting of the mantle? *Journal of Volcanology and Geothermal Research*, *185*(1-2), 116–122. doi: 10.1016/j.jvolgeores.2008.11.027

Elkins-Tanton, L. T., Hess, P. C., & Parmentier, E. M. (2005). Possible formation of ancient crust on Mars through magma ocean processes. *Journal of Geophysical Research: Planets*, *110*(E12), E12S01. doi: 10.1029/2005JE002480

Elkins-Tanton, L. T., Parmentier, E. M., & Hess, P. C. (2003). Magma ocean fractional crystallization and cumulate overturn in terrestrial planets: Implications for Mars. *Meteoritics and Planetary Science*, *38*(12), 1753–1771. doi: 10.1111/j.1945-5100.2003.tb00013.x

Farley, K. A., Stack, K. M., Shuster, D. L., Horgan, B. H. N., Hurowitz, J. A., Tarnas, J. D., ... Zorzano, M.-P. (2022). Aqueously altered igneous rocks sampled on the floor of Jezero crater, Mars. *Science*, *0*(0), eabo2196. doi: 10.1126/science.abo2196

Ferdous, J., Brandon, A., Peslier, A., & Pirotte, Z. (2017). Evaluating Crustal Contributions to Enriched Shergottites from the Petrology, Trace Elements, and Rb-Sr and Sm-Nd Isotope Systematics of Northwest Africa 856. *Geochimica et Cosmochimica Acta*. doi: 10.1016/j.gca.2017.05.032

Filiberto, J. (2017). Geochemistry of Martian basalts with constraints on magma genesis. *Chemical Geology*, *466*, 1–14. doi: https://doi.org/10.1016/j.chemgeo.2017.06.009

Filiberto, J., & Dasgupta, R. (2011). Fe2+-Mg partitioning between olivine and basaltic melts: Applications to genesis of olivine-phyric shergottites and conditions of melting in the Martian interior. *Earth and Planetary Science Letters*, *304*(3-4), 527–537. doi: 10.1016/j.epsl.2011.02.029

Filiberto, J., & Dasgupta, R. (2015). Constraints on the depth and thermal vigor of melting in the Martian mantle. *Journal of Geophysical Research: Planets*, 2014JE004745. doi: 10.1002/2014JE004745

Filiberto, J., Dasgupta, R., Kiefer, W. S., & Treiman, A. H. (2010). High pressure, near-liquidus phase equilibria of the Home Plate basalt Fastball and melting in the Martian mantle. *Geophysical Research Letters*, *37*(13), 1–4. doi: 10.1029/2010GL043999

Filiberto, J., Musselwhite, D. S., Gross, J., Burgess, K., Le, L., & Treiman, A. H. (2010). Experimental petrology, crystallization history, and parental magma characteristics of olivine-phyric shergottite NWA 1068: Implications for the petrogenesis of "enriched" olivine-phyric shergottites. *Meteoritics and Planetary Science*, *45*(8), 1258–1270. doi: 10.1111/j.1945-5100.2010.01080.x

Filiberto, J., Treiman, A. H., & Le, L. (2008). Crystallization experiments on a Gusev Adirondack basalt composition. *Meteoritics and Planetary Science*, *43*(7), 1137–1146.

Goodrich, C. A., Treiman, A. H., Filiberto, J., Gross, J., & Jercinovic, M. (2013).

K2O-rich trapped melt in olivine in the Nakhla meteorite: Implications for petrogenesis of nakhlites and evolution of the Martian mantle. *Meteoritics and Planetary Science*, *48*(12), 2371–2405. doi: 10.1111/maps.12226

Greeley, R., Foing, B. H., McSween, H. Y., Neukum, G., Pinet, P., van Kan, M., ... Zegers, T. E. (2005). Fluid lava flows in Gusev crater, Mars. *Journal of Geophysical Research E: Planets*, *110*(5), 1–6. doi: 10.1029/2005JE002401

Greshake, A., Fritz, J., & Stoffler, D. (2004). Petrology and shock metamorphism of the olivine-phyric shergottite Yamato 980459: Evidence for a two-stage cooling and a single-stage ejection history. *Geochimica Et Cosmochimica Acta*, *68*(10), 2359–2377. doi: 10.1016/j.gca.2003.11.022

Gross, J., Treiman, A. H., Filiberto, J., & Herd, C. D. K. (2011). Primitive olivine-phyric shergottite NWA 5789: Petrography, mineral chemistry, and cooling history imply a magma similar to Yamato-980459. *Meteoritics and Planetary Science*, *133*(1), no–no. doi: 10.1111/j.1945-5100.2010.01152.x

He, Q., Xiao, L., Hsu, W., Balta, J. B., McSween, H. Y., & Liu, Y. (2013). The water content and parental magma of the second chassignite NWA 2737: Clues from trapped melt inclusions in olivine. *Meteoritics and Planetary Science*, *48*(3), 474–492. doi: 10.1111/maps.12073

Huang, Q., Schmerr, N. C., King, S. D., Kim, D., Rivoldini, A., Plesa, A. C., ... Banerdt, W. B. (2022). Seismic detection of a deep mantle discontinuity within Mars by InSight. *Proceedings of the National Academy of Sciences of the United States of America*, *119*(42), e2204474119. doi: 10.1073/pnas.2204474119

Humayun, M., Nemchin, A., Zanda, B., Hewins, R. H., Grange, M., Kennedy, A., ... Deldicque, D. (2013). Origin and age of the earliest Martian crust from meteorite NWA 7533. *Nature*, *503*(7477), 513–516. doi: 10.1038/nature12764

Johnston, D. H., & Toksöz, M. N. (1977). Internal structure and properties of Mars. *Icarus*, *32*(1), 73–84. doi: 10.1016/0019-1035(77)90050-1

Katz, R. F., Spiegelman, M., & Langmuir, C. H. (2003). A new parameterization of hydrous mantle melting. *Geochemistry, Geophysics, Geosystems*, *4*(9), 1073. doi: 10.1029/2002GC000433

Khan, A., Ceylan, S., van Driel, M., Giardini, D., Lognonné, P., Samuel, H., ... Banerdt, W. B. (2021). Upper mantle structure of Mars from InSight seismic data. *Science*, *373*(6553), 434–438. doi: 10.1126/science.abf2966

Khan, A., Sossi, P. A., Liebske, C., Rivoldini, A., & Giardini, D. (2022). Geophysical and cosmochemical evidence for a volatile-rich Mars. *Earth and Planetary Science Letters*, *578*, 117330. doi: 10.1016/j.epsl.2021.117330

Kruijer, T. S., Kleine, T., Borg, L. E., Brennecka, G. A., Irving, A. J., Bischoff, A., & Agee, C. B. (2017). The early differentiation of Mars inferred from Hf–W chronometry. *Earth and Planetary Science Letters*. doi: 10.1016/j.epsl.2017.06.047

Lagain, A., Benedix, G. K., Servis, K., Baratoux, D., Doucet, L. S., Rajšic, A., ... Miljković, K. (2021). The Tharsis mantle source of depleted shergottites revealed by 90 million impact craters. *Nature Communications*, *12*(1), 1–9. doi: 10.1038/s41467-021-26648-3

Lagain, A., Bouley, S., Zanda, B., Miljković, K., Rajšić, A., Baratoux, D., ... Bland, P. A. (2022). Early crustal processes revealed by the ejection site of the oldest martian meteorite. *Nature Communications*, *13*(1), 3782. doi: 10.1038/s41467-022-31444-8

Lee, C.-T. A., Luffi, P., Plank, T., Dalton, H., & Leeman, W. P. (2009). Constraints on the depths and temperatures of basaltic magma generation on Earth and other terrestrial planets using new thermobarometers for mafic magmas. *Earth and Planetary Science Letters*, *279*(1–2), 20–33. doi: http://dx.doi.org/10.1016/j.epsl.2008.12.020

Lodders, K., & Fegley, B. (1997). An oxygen isotope model for the composition of

Mars. *Icarus*, *126*(2), 373–394. doi: 10.1006/icar.1996.5653

Longhi, J., Knittle, E., Holloway, J. R., & Waenke, H. (1992). The bulk composition, mineralogy and internal structure of Mars. In *Mars* (pp. 184–208). AA(Lamont-Doherty Earth Observatory), AB(University of California, Santa Cruz), AC(Arizona State University), AD(Max-Planck-Institute for Chemistry, Mainz).

Matzen, A. K., Woodland, A., Beckett, J. R., & Wood, B. J. (2022). Oxidation state of iron and Fe-Mg partitioning between olivine and basaltic martian melts. *American Mineralogist*, *107*(7), 1442–1452. doi: 10.2138/am-2021-7682

McCubbin, F. M., Boyce, J. W., Srinivasan, P., Santos, A. R., Elardo, S. M., Filiberto, J., ... Shearer, C. K. (2016). Heterogeneous distribution of H2O in the Martian interior: Implications for the abundance of H2O in depleted and enriched mantle sources. *Meteoritics and Planetary Science*, *51*(11), 2036–2060. doi: 10.1111/maps.12639

McCubbin, F. M., Elardo, S. M., Shearer, C. K., Smirnov, A., Hauri, E. H., & Draper, D. S. (2013). A petrogenetic model for the comagmatic origin of chassignites and nakhlites: Inferences from chlorine-rich minerals, petrology, and geochemistry. *Meteoritics and Planetary Science*, *48*(5), 819–853. doi: 10.1111/maps.12095

McFarlane, C. R. M., & Spray, J. G. (2022). The Los Angeles martian diabase: Phosphate U-Th-Pb geochronology and mantle source constraints. *Geochimica et Cosmochimica Acta*, *326*, 166–179. doi: https://doi.org/10.1016/j.gca.2022.04.006

McSween, H. Y., Ruff, S. W., Morris, R. V., Bell, J. F., Herkenhoff, K., Gellert, R., ... Schmidt, M. (2006). Alkaline volcanic rocks from the Columbia Hills, Gusev crater, Mars. *Journal of Geophysical Research E: Planets*, *111*(9), n/a–n/a. doi: 10.1029/2006JE002698

McSween, H. Y., Wyatt, M. B., Gellert, R., Bell, I. F., Morris, R. V., Herkenhoff, K. E., ... Zipfel, J. (2006). Characterization and petrologic interpretation of olivine-rich basalts at Gusev Crater, Mars. *Journal of Geophysical Research E: Planets*, *111*(2), 1–17. doi: 10.1029/2005JE002477

Ming, D. W., Gellert, R., Morris, R. V., Arvidson, R. E., Brückner, J., Clark, B. C., ... Zipfel, J. (2008). Geochemical properties of rocks and soils in Gusev Crater, Mars: Results of the Alpha Particle X-Ray Spectrometer from Cumberland Ridge to Home Plate. *Journal of Geophysical Research: Planets*, *113*(E12), E12S39. doi: 10.1029/2008JE003195

Misawa, K. (2004). The Yamato 980459 olivine-phyric shergottite consortium. *Antartic Meteorite Research*, *17*, 1–12.

Monders, A. G., Médard, E., & Grove, T. L. (2007). Phase equilibrium investigations of the Adirondack class basalts from the Gusev plains, Gusev crater, Mars. *Meteoritics and Planetary Science*, *42*(1), 131–148. doi: 10.1111/j.1945-5100.2007.tb00222.x

Moser, D. E., Chamberlain, K. R., Tait, K. T., Schmitt, A. K., Darling, J. R., Barker, I. R., & Hyde, B. C. (2013). Solving the Martian meteorite age conundrum using micro-baddeleyite and launch-generated zircon. *Nature*, *499*(7459), 454–457. doi: 10.1038/nature12341

Musselwhite, D. S., Dalton, H. A., Kiefer, W. S., & Treiman, A. H. (2006). Experimental petrology of the basaltic shergottite Yamato-980459: Implications for the thermal structure of the Martian mantle. *Meteoritics and Planetary Science*, *41*(9), 1271–1290. doi: 10.1111/j.1945-5100.2006.tb00521.x

Nyquist, L. E., Shih, C. Y., Mccubbin, F. M., Santos, A. R., Shearer, C. K., Peng, Z. X., ... Agee, C. B. (2016). Rb-Sr and Sm-Nd isotopic and REE studies of igneous components in the bulk matrix domain of Martian breccia Northwest Africa 7034. *Meteoritics and Planetary Science*, *51*(3), 483–498. doi: 10.1111/maps.12606

Ostwald, A., Udry, A., Payré, V., Gazel, E., & Wu, P. (2022). The role of assimilation and fractional crystallization in the evolution of the Mars crust. *Earth and Planetary Science Letters*, *585*, 117514. doi: 10.1016/j.epsl.2022.117514

Payré, V., Siebach, K. L., Dasgupta, R., Udry, A., Rampe, E. B., & Morrison, S. M. (2020). Constraining Ancient Magmatic Evolution on Mars Using Crystal Chemistry of Detrital Igneous Minerals in the Sedimentary Bradbury Group, Gale Crater, Mars. *Journal of Geophysical Research: Planets*, *125*(8), e2020JE006467. doi: 10.1029/2020JE006467

Peslier, A. H., Hnatyshin, D., Herd, C. D. K., Walton, E. L., Brandon, A. D., Lapen, T. J., & Shafer, J. T. (2010). Crystallization, melt inclusion, and redox history of a Martian meteorite: Olivine-phyric shergottite Larkman Nunatak 06319. *Geochimica et Cosmochimica Acta*, *74*(15), 4543–4576. doi: 10.1016/j.gca.2010.05.002

Plesa, A. C., Wieczorek, M., Knapmeyer, M., Rivoldini, A., Walterová, M., & Breuer, D. (2022). Interior dynamics and thermal evolution of Mars – a geodynamic perspective. In *Advances in geophysics* (Vol. 63, pp. 179–230). Elsevier. doi: 10.1016/bs.agph.2022.07.005

Schmidt, M. E., Campbell, J. L., Gellert, R., Perrett, G. M., Treiman, A. H., Blaney, D. L., ... Wiens, R. C. (2014). Geochemical diversity in first rocks examined by the Curiosity Rover in Gale Crater: Evidence for and significance of an alkali and volatile-rich igneous source. *Journal of Geophysical Research: Planets*, n/a–n/a. doi: 10.1002/2013JE004481

Schmidt, M. E., & McCoy, T. J. (2010). The evolution of a heterogeneous Martian mantle: Clues from K, P, Ti, Cr, and Ni variations in Gusev basalts and shergottite meteorites. *Earth and Planetary Science Letters*, *296*(1-2), 67–77. doi: 10.1016/j.epsl.2010.04.046

Shafer, J. T., Brandon, A. D., Lapen, T. J., Righter, M., Peslier, A. H., & Beard, B. L. (2010). Trace element systematics and 147Sm-143Nd and 176Lu-176Hf ages of Larkman Nunatak 06319: Closed-system fractional crystallization of an enriched shergottite magma. *Geochimica et Cosmochimica Acta*, *74*(24), 7307–7328. doi: 10.1016/j.gca.2010.09.009

Shih, C.-Y., Nyquist, L., Wiesmann, H., Reese, Y., & Misawa, K. (2005). Rb-Sr and Sm-Nd dating of olivine-phyric shergottite Yamato 980459: Petrogenesis of depleted shergottites. *Antarctic meteorite research*, *18*, 46–65.

Shirai, N., & Ebihara, M. (2004). Chemical characteristics of a Martian meteorite, Yamato 980459. *Antartic Meteorite Research*, *17*, 55–67.

Smith, D., Griffin, W. L., & Ryan, C. G. (1993). Compositional evolution of high-temperature sheared lherzolite PHN 1611. *Geochimica et Cosmochimica Acta*, *57*(3), 605–613. doi: 10.1016/0016-7037(93)90371-3

Squyres, S. W., Aharonson, O., Clark, B. C., Cohen, B. a., Crumpler, L., de Souza, P. a., ... Yen, A. (2007). Pyroclastic activity at Home Plate in Gusev Crater, Mars. *Science*, *316*(5825), 738–42. doi: 10.1126/science.1139045

Symes, S. J. K., Borg, L. E., Shearer, C. K., & Irving, A. J. (2008). The age of the martian meteorite Northwest Africa 1195 and the differentiation history of the shergottites. *Geochimica et Cosmochimica Acta*, *72*(6), 1696–1710. doi: 10.1016/j.gca.2007.12.022

Udry, A., & Day, J. M. D. (2018). 1.34 billion-year-old magmatism on Mars evaluated from the co-genetic nakhlite and chassignite meteorites. *Geochimica et Cosmochimica Acta*, *238*, 292–315. doi: 10.1016/j.gca.2018.07.006

Udry, A., Gazel, E., & McSween, H. Y. (2018). Formation of Evolved Rocks at Gale Crater by Crystal Fractionation and Implications for Mars Crustal Composition. *Journal of Geophysical Research: Planets*, *123*(6), 1525–1540. doi: 10.1029/2018JE005602

Udry, A., Lunning, N. G., McSween Jr, H. Y., & Bodnar, R. J. (2014). Petrogenesis of a vitrophyre in the martian meteorite breccia NWA 7034. *Geochimica*

et Cosmochimica Acta, *141*(0), 281–293. doi: http://dx.doi.org/10.1016/j.gca.2014.06.026

Wieczorek, M. A., Broquet, A., McLennan, S. M., Rivoldini, A., Golombek, M., Antonangeli, D., ... Banerdt, W. B. (2022). InSight Constraints on the Global Character of the Martian Crust. *Journal of Geophysical Research: Planets*, *127*(5), 1–35. doi: 10.1029/2022JE007298

Wiens, R. C., Udry, A., Beyssac, O., Quantin-Nataf, C., Mangold, N., Cousin, A., ... Null, N. (2022). Compositionally and density stratified igneous terrain in Jezero crater, Mars. *Science Advances*, *8*(34), eabo3399. doi: 10.1126/sciadv.abo3399

Wittmann, A., Korotev, R. L., Jolliff, B. L., Irving, A. J., Moser, D. E., Barker, I., & Rumble, D. (2015). Petrography and composition of Martian regolith breccia meteorite Northwest Africa 7475. *Meteoritics and Planetary Science*, *50*(2), 326–352. doi: 10.1111/maps.12425

Wu, Y., Hsu, W., Li, Q.-L., Che, X., & Liao, S. (2021). Heterogeneous martian mantle: Evidence from petrology, mineral chemistry, and in situ U-Pb chronology of the basaltic shergottite Northwest Africa 8653. *Geochimica et Cosmochimica Acta*, *309*, 352–365. doi: https://doi.org/10.1016/j.gca.2021.05.011

Yoshizaki, T., & McDonough, W. F. (2020). The composition of Mars. *Geochimica et Cosmochimica Acta*, *273*, 137–162. doi: 10.1016/j.gca.2020.01.011

Figure 1.

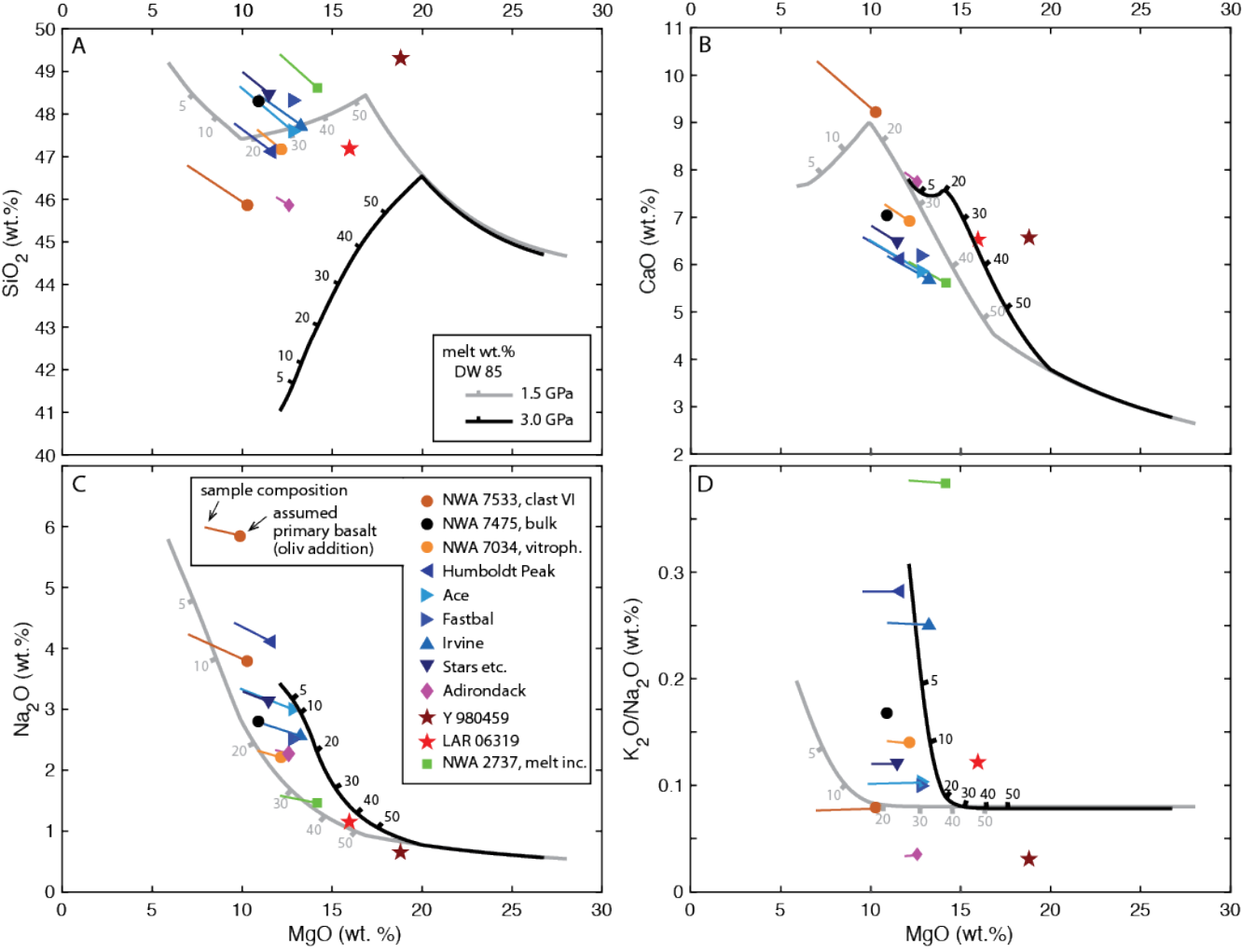
A
B
C
D
SiO2 (wt.%)
CaO (wt.%)
Na2O (wt.%)
K2O/Na2O (wt.%)
MgO (wt. %)
MgO (wt.%)
melt wt.%
DW 85
1.5 GPa
3.0 GPa
sample composition
assumed primary basalt (oliv addition)
NWA 7533, clast VI
NWA 7475, bulk
NWA 7034, vitroph.
Humboldt Peak
Ace
Fastbal
Irvine
Stars etc.
Adirondack
Y 980459
LAR 06319
NWA 2737, melt inc.

Figure 2.

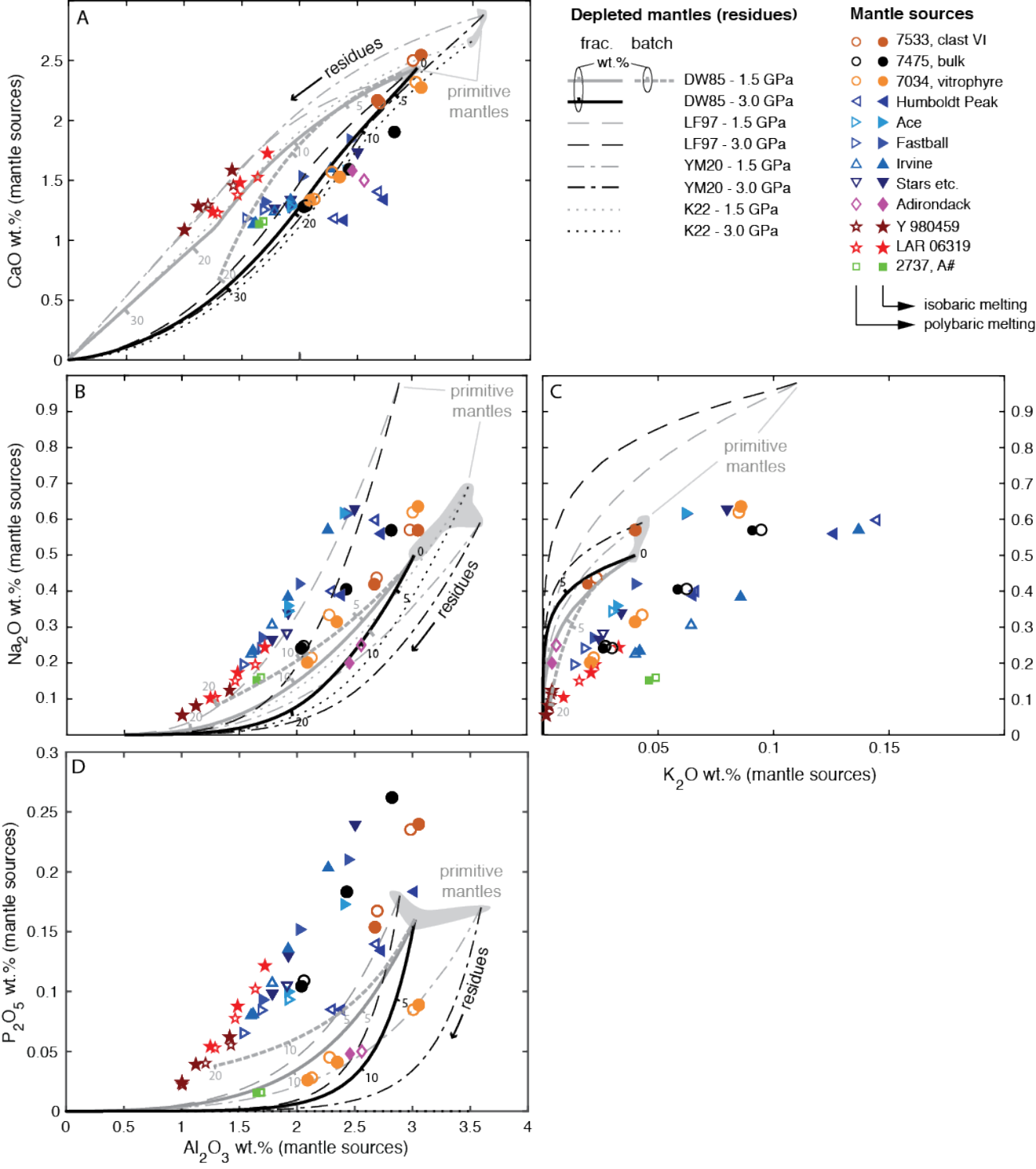
A
B
C
D
CaO wt.% (mantle sources)
Na2O wt.% (mantle sources)
K2O wt.% (mantle sources)
P2O5 wt.% (mantle sources)
Al2O3 wt.% (mantle sources)
residues
primitive mantles
Depleted mantles (residues)
frac.
batch
wt.%
DW85 - 1.5 GPa
DW85 - 3.0 GPa
LF97 - 1.5 GPa
LF97 - 3.0 GPa
YM20 - 1.5 GPa
YM20 - 3.0 GPa
K22 - 1.5 GPa
K22 - 3.0 GPa
Mantle sources
7533, clast VI
7475, bulk
7034, vitrophyre
Humboldt Peak
Ace
Fastball
Irvine
Stars etc.
Adirondack
Y 980459
LAR 06319
2737, A#
isobaric melting
polybaric melting

Figure 3.

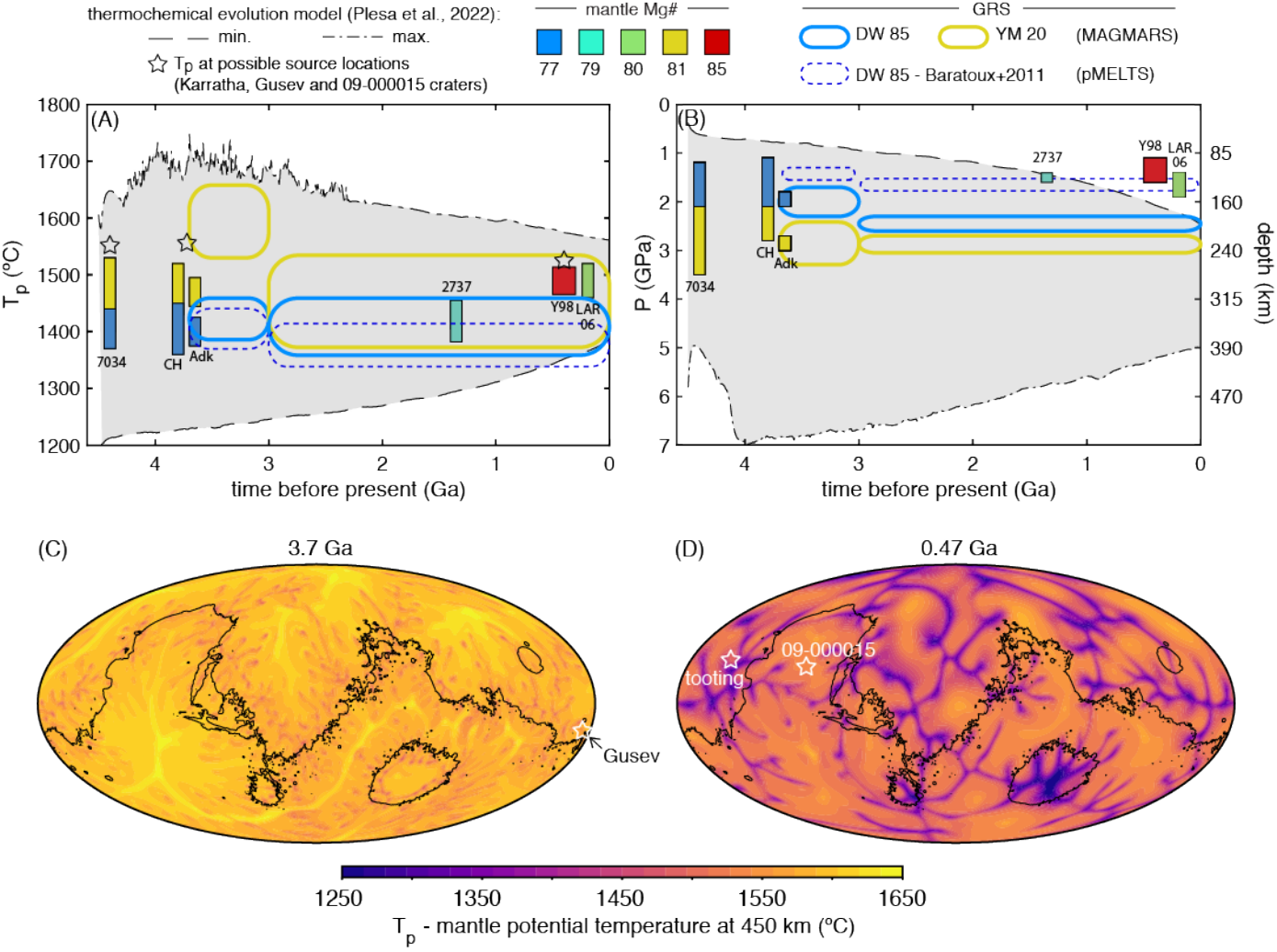
thermochemical evolution model (Plesa et al., 2022):
min.
max.
Tp at possible source locations
(Karratha, Gusev and 09-000015 craters)
mantle Mg#
77
79
80
81
85
GRS
DW 85
YM 20
(MAGMARS)
DW 85 - Baratoux+2011
(pMELTS)
(A)
Tp (°C)
time before present (Ga)
7034
CH
Adk
2737
Y98
LAR 06
(B)
P (GPa)
depth (km)
(C)
3.7 Ga
Gusev
(D)
0.47 Ga
09-000015
tooting
1250
1350
1450
1550
1650
Tp - mantle potential temperature at 450 km (°C)

Geophysical Research Letters

Supporting Information for

The temperature and composition of the mantle sources of Martian basalts

Max Collinet[1], Ana-Catalina Plesa[1], Thomas Ruedas[2,1], Sabrina Schwinger[1], Doris Breuer[1]

[1]German Aerospace Center (DLR), Institute of Planetary Research, Rutherfordstraße 2, 12489 Berlin, Germany, [2]Museum für Naturkunde Berlin, Impact and Meteorite Research, Invalidenstraße 43, 10115 Berlin, Germany

Contents of this file

1. Text S1 and associated figures S1 and S2: discussion of non-uniqueness and model uncertainties
2. Figure S3: temperature profile below the possible locations of primitive Martian basalts

Additional Supporting Information (Files uploaded separately)

1. Supplementary Tables S1–S3 (with submission)
2. MAGMARS results used in figure 3 to match the GRS volcanic provinces of Baratoux et al. (2011) (data repository)
3. MAGMARS scripts and files used to produce figure S1–S2 (data repository)

   data repository: https://doi.org/10.5281/zenodo.7691390

S1 Non-uniqueness and model uncertainties

MAGMARS uncertainties are discussed in detail in section 3.2 of Collinet et al. (2021) and propagated by combining analytical, experimental, and model uncertainties. They are provided as fixed average uncertainties for the composition of melts produced by melting any mantle composition, at any pressure and temperature: $\pm$ 1.3 wt.% SiO_2, 0.21 wt.% TiO_2, 0.38 wt.% Al_2O_3, 0.11 wt.% Cr_2O_3, 0.85 wt.% FeO, 0.06 wt.% MnO, 0.75 wt.% MgO, 0.61 wt.% CaO, 0.28 wt.% Na_2O, 0.12 wt.% K_2O, 0.12 wt.% P_2O_5, for lherzolite melting. To quantify the uncertainties on the mantle composition and melting conditions that can produce a specific primary basalt, we run a large number of simulations while varying systematically the parameter space (black contours in Figure S1). We retain only the simulations that produce a melt identical to the basalt Fastball (representative example) within the model uncertainties stated above (blue circles). Figure S1 can be compared to Figure 2 and shows that despite the substantial uncertainties associated with the method, the conclusions of the study remain unchanged.

Another large set of simulations is filtered assuming that the model uncertainties are smaller than reported in Collinet et al. (2021) (Figure S2). While it is possible that the MAGMARS model uncertainties are overly conservative, the goal here is simply to isolate model uncertainties and non-uniqueness. Even assuming a small model uncertainty, there is a large array of possible mantle sources and melting conditions that can produce nearly identical basaltic melts (the composition of Fastball in this case).
For a given basaltic melt (e.g., Fastball), the most refractory mantle sources are associated with the lowest melt fraction and lowest mantle temperatures due to the smaller release of latent heat of melting (Fig. S1a,b). To produce the same average basaltic liquid by polybaric melting as by isobaric melting, melting must start deeper and extend to a shallower region of the mantle, where the solidus temperature is low. The T_{p} is therefore lower compared to the isobaric case (Table S2, Fig. S1a, S2a, also see Fig. 2 in Collinet et al., 2021).

References

Baratoux, D., Toplis, M. J., Monnereau, M., and Gasnault, O. (2011). Thermal history of Mars inferred from orbital geochemistry of volcanic provinces. *Nature*, 472(7343):338–41.

Collinet, M., Plesa, A., Grove, T. L., Schwinger, S., Ruedas, T., and Breuer, D. (2021). MAGMARS: A Melting Model for the Martian Mantle and FeO-Rich Peridotite. *Journal of Geophysical Research: Planets*, 126(12):e2021JE006985.

Lagain, A., Benedix, G. K., Servis, K., Baratoux, D., Doucet, L. S., Rajšic, A., Devillepoix, H. A. R., Bland, P. A., Towner, M. C., Sansom, E. K., and Miljković, K. (2021). The Tharsis mantle source of depleted shergottites revealed by 90 million impact craters. *Nature Communications*, 12(1):1–9.

Lagain, A., Bouley, S., Zanda, B., Miljković, K., Rajšić, A., Baratoux, D., Payré, V., Doucet, L. S., Timms, N. E., Hewins, R., Benedix, G. K., Malarewic, V., Servis, K., and Bland, P. A. (2022). Early crustal processes revealed by the ejection site of the oldest martian meteorite. *Nature Communications*, 13(1):3782.

Plesa, A. C., Wieczorek, M., Knapmeyer, M., Rivoldini, A., Walterová, M., and Breuer, D. (2022). Interior dynamics and thermal evolution of Mars – a geodynamic perspective. In *Advances in Geophysics*, volume 63 of *Advances in Geophysics*, pages 179–230. Elsevier.

Ruedas, T. and Breuer, D. (2017). On the relative importance of thermal and chemical buoyancy in regular and impact-induced melting in a Mars-like planet. *Journal of Geophysical Research: Planets*, 122(7):1554–1579.

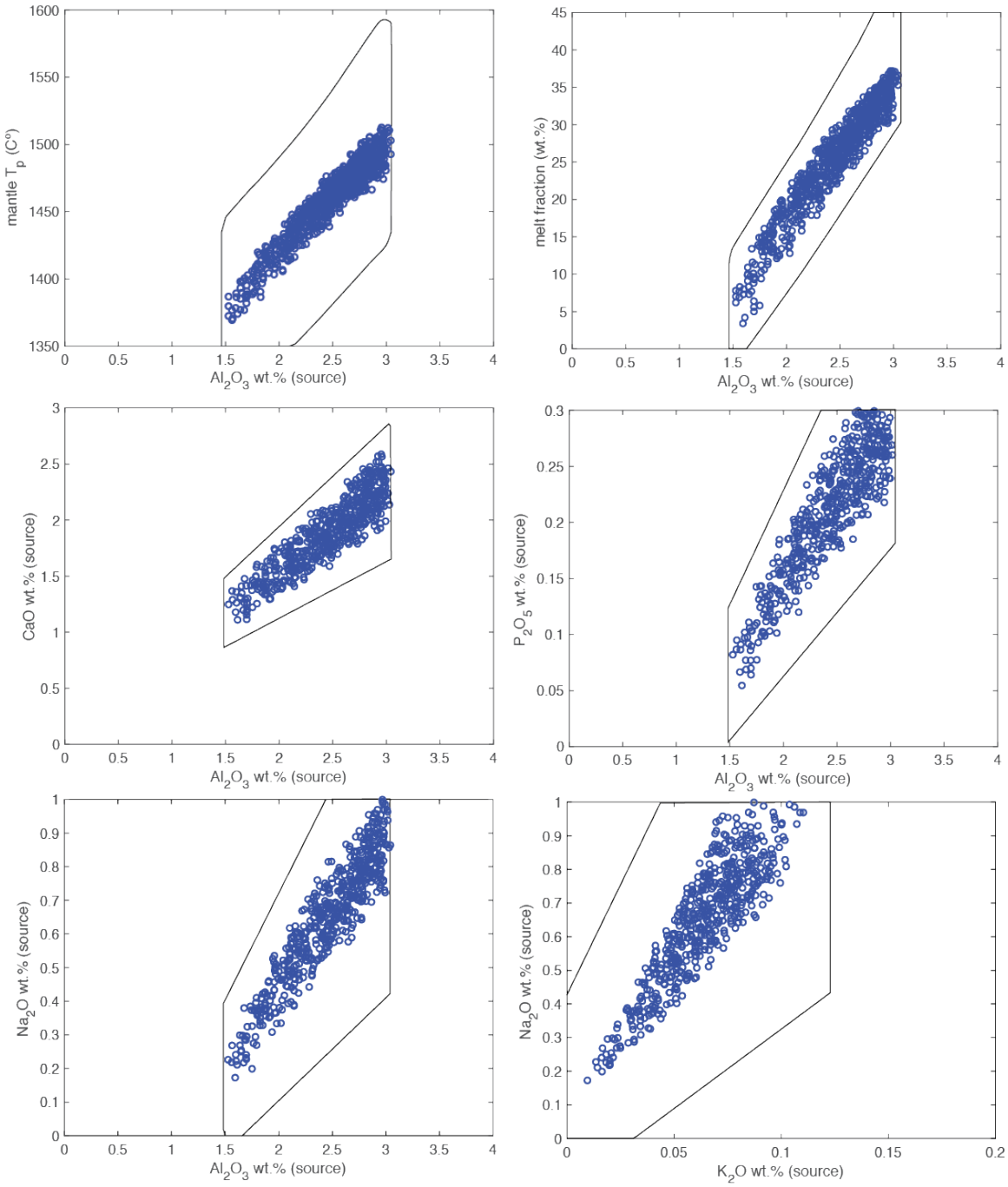

Figure S1: MAGMARS simulations able to reproduce the composition of Fastball (blue circle) assuming the average model uncertainty of Collinet et al. (2021): ± 1.3 wt.% SiO_2, 0.21 wt.% TiO_2, 0.38 wt.% Al_2O_3, 0.11 wt.% Cr_2O_3, 0.85 wt.% FeO, 0.06 wt.% MnO, 0.75 wt.% MgO, 0.61 wt.% CaO, 0.28 wt.% Na_2O, 0.12 wt.% K_2O, 0.12 wt.% P_2O_5. The black envelope represents the conditions sampled by 105000 MAGMARS simulations.

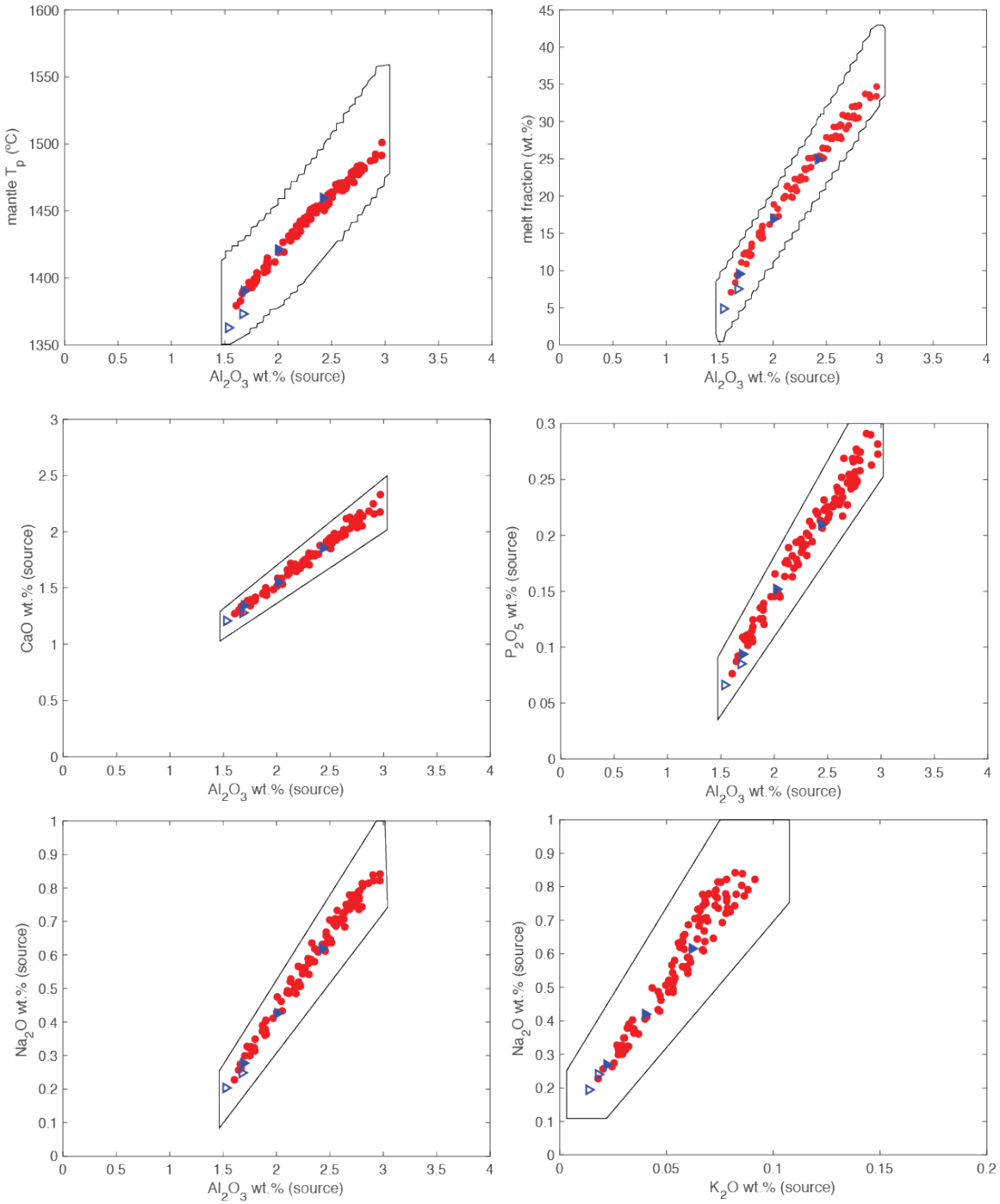

Figure S2: MAGMARS simulations able to reproduce the composition of Fastball assuming a low uncertainty of ± 0.5 wt.% SiO_2, 0.05 wt.% TiO_2, 0.15 wt.% Al_2O_3, 0.11 Cr_2O_3, 0.25 wt.% FeO, 0.06 MnO, 0.25 wt.% MgO, 0.15 wt.% CaO, 0.07 wt.% Na_2O, 0.03 wt.% K_2O, 0.05 wt.% P_2O_5 (red circles). The open and closed blue triangles represent the sample sources reported in Figure 2 and Table S2. The black envelope represents the conditions sampled by 375000 MAGMARS simulations.

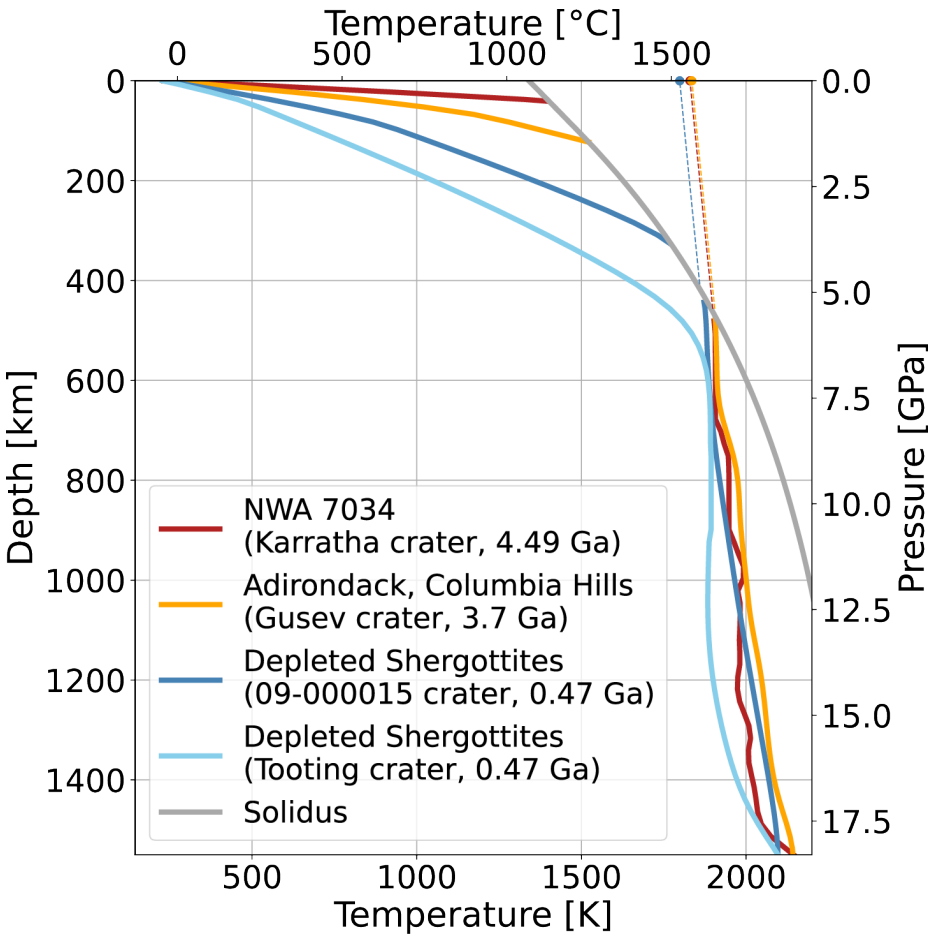

Figure S3: Temperature profiles of the mantle below Gusev crater, and the possible location of the sources of depleted shergottites (09-000015, Tooting; Lagain et al. (2021)) and NWA 7034 (Karratha; Lagain et al. (2022)) at the time of their crystallization, from the thick-crust model of Plesa et al. (2022). The mantle below Tooting crater does not reach the solidus of Ruedas and Breuer (2017) (grey line). Below the other 3 craters, the solidus is crossed at ∼5 GPa and the mantle potential temperatures are nearly identical (filled circles on the upper temperature axis): 1556 ℃ (Karratha), 1562℃ (Gusev) and 1525 ℃ (09-000015).